A. Mancisidor, A. Zubizarreta, I. Cabanes, P. Bengoa, M. Marcos and J. H. Jung, "*Enhanced force control using force estimation and nonlinearity compensation for the Universal Haptic Pantograph,*" **2015 IEEE/RSJ International Conference on Intelligent Robots and Systems (IROS), Hamburg, Germany, 2015,** pp. 5599-5604, https://doi.org/10.1109/IROS.2015.7354171

Enhanced force control using force estimation and nonlinearity compensation for the Universal Haptic Pantograph

Aitziber Mancisidor[1], Asier Zubizarreta[1], Itziar Cabanes[1], Pablo Bengoa[1], Marga Marcos[1] and Je Hyung Jung[2]

***Abstract*— The design of a stable and robust force controller is one of the most important and difficult tasks in rehabilitation robotics. In previous works, the Universal Haptic Pantograph (UHP) was presented as an alternative to conventional arm rehabilitation after a stroke. This robot is composed by a Series Elastic Actuator (SEA) and a Pantograph.**

In this work an enhanced force control for the UHP is presented. The proposed controller uses the robot model to estimate the contact force without direct measurement and to compensate nonlinearities in the actuators. In order to prove the effectiveness of the approach, several tests are carried out in simulation and experimentally. Results reveal that mean of tracking errors between desired and actual force is smaller than 0.1 N, which is significantly improved compare to that (around 2.5 N) shown in previous results of UHP, indicating that the proposed force control is likely to enhance haptic performance of the UHP.

I. INTRODUCTION

In the last few years, stroke has become one of the most common diseases. A conservative estimation states that 17 million new stroke cases are produced every year. Although one third of patients die, most of them survive due to new fast acting protocols. However, survivors have to cope with the effects of the stroke, which include some functional limitations. It is estimated that nearly 33 million of people have to deal currently with stroke sequels [1], [2].

One of the more important and frequent sequel is hemiplegia, i.e, the complete or partial paralysis of half of the body. Therefore, it is essential to follow a rehabilitation programme to recover the lost mobility, so that the patient can perform daily tasks with the greatest possible autonomy.

In view of this situation, robotics is proposed as an interesting alternative that can bring several benefits to the rehabilitation process. Longer treatments, patient adapted intensity levels, repeatability and accuracy, motivation increased by the use of virtual reality software, cost-effectiveness, and the possibility to analyze the patient progress, are some of the benefits that robotic technology provides to rehabilitation processes.

In the past few years several works have proposed robots to rehabilitate upper [3], [4], and lower [5], [6] limbs. As most daily tasks are performed with the arms, their rehabilitation is critical to enhancing the autonomy of the patient after a stroke. For that reason, most recent works are focused on upper limbs rehabilitation devices, which is also the scope of this work. Although there are some portable devices such as RUPERT [7], most of them are not portable and require a fixed support [8] due to the size and need of power of actuators, their weight, safety and adaptability.

One of the most important issues in rehabilitation robotics is the design of control approaches for proper and safe user interaction. However, in addition to the complex structure of most rehabilitation robots, unknown user interaction has to be dealt with. Hence, robot motion will be affected not only by the actuators, but also by the forces exerted by the patient. Therefore, the common position control strategies are inadequate as they do not consider the dynamics of the interaction between the robot and the user [9].

Advanced control algorithms that combine motion and force measurements have to be implemented to deal with this interaction so that the robot can control the force exerted to the patient while allowing its motion to perform rehabilitation tasks. In the literature, several approaches have been proposed to implement patient-robot interaction in rehabilitation robotics. One of the most used approach is impedance control [10], [11], in which the relationship between position and force can be controlled, adapting it to the state of the patient [12], [13]. However, other control approaches such as force control [14], computed torque control [15], admittance control [8] or algorithms using EMG signals [16], [17] have also been used based on the particular requirements of the robot structure.

In this work an enhanced force control architecture is presented for the Universal Haptic Pantograph (UHP), a robot for comprehensive upper limbs movement training after stroke [18]. The UHP is composed of 2 Series Elastic Actuators (SEAs) and a pantograph structure that interacts with the user. Although the force control performance presented in previous studies [19] seems to be acceptable, from the control point of view there is still room to improve the performance for the sake of more transparent haptic interaction between user and robot. In the proposed force control architecture, interaction force is estimated using the robot model instead

*This work was supported in part by the Basque Country Governments (GV/EJ) under grant PRE-2014-1-152, Spanish Ministry of Economy and Competitiveness' MINECO & FEDER inside the DPI-2012-328822 project, Basque Country Governments IT719-13 project, UPV/EHU's UFI11/25 project, Euskampus, FIK and Spanish Ministry of Science and Innovation PDI-020100-2009-21 project.

[1] A. Mancisidor, A. Zubizarreta, I. Cabanes, P. Bengoa and M. Marcos are with the Department of Automatics and System Engineering, University of the Basque Country (UPV/EHU), Bilbao 48013, Spain asier.zubizarreta@ehu.eus

[2] Je Hyung Jung is with the Rehabilitation Area, Health Division, TECNALIA Research and Innovation, Mikeletegi Pasealekua, 1-3 E-20009 Donostia-San Sebastian, Spain. jehyung.jung@tecnalia.com

of directly measuring it and compensators are incorporated to reduce the effects of nonlinearities in the actuator.

The rest of the article is structured as follows. In Section II, the UHP robot is described and its model detailed; in section III the force controller is presented and analyzed. Section IV analyzes the performance of the force controller in several simulated and experimental case studies. Finally, the most important ideas are summarized in the conclusions.

II. UNIVERSAL HAPTIC PANTOGRAPH

The Universal Haptic Pantograph (UHP) is an upper limbs rehabilitation robot [18], [19] which has the ability to modify its mechanical structure thanks to its three lockable/unlockable joints, allowing to use the same structure to perform different rehabilitation exercises in the upper limbs.

This work is focused in the ARM mode of the robot, which is used to mainly rehabilitate elbow and shoulder by means of nearly planar motions of arm extension or reach in the four possible directions (backward, forward, right and left).

The robot is divided into two parts: the drive system SEA (Series Elastic Actuator) and the pantograph, which interacts with the patient (Fig. 1). Both sides are connected, so there exist a force $\mathbf{F_{Trans}}$ and movement $\mathbf{x_{Trans}}$ transmission between them. In addition, the robot motion is caused by two rotative motors which apply a torque $\boldsymbol{\tau_m}$ to the SEA and the force $\mathbf{F_{Cont}}$ and motion $\mathbf{x_{Cont}}$ exerted by the patient .

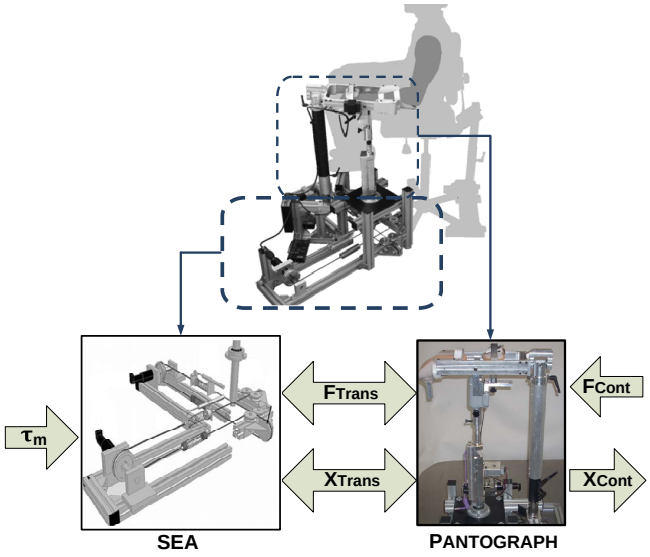

Fig. 1. UHP Block Diagram.

The SEA is composed by two motors (m_1, m_2) and four springs (S_A, S_B, S_C, S_D) and is connected to the Pantograph in point $\mathbf{P_x}$ (Fig. 2). All elements are connected by cables which transmit force and motion. For instance, the motor torque exerted by m_1 is transmitted to the springs S_A and S_C, and this force is transmitted to the pantograph by means of the connection point $\mathbf{P_x}$ (Figs. and 2 and 3).

The equilibrium position of the UHP is achieved when the pantograph arm is in vertical position, defining the origin of the base reference frame $\mathbf{P_0}$ (Fig. 3). Note that the pantograph

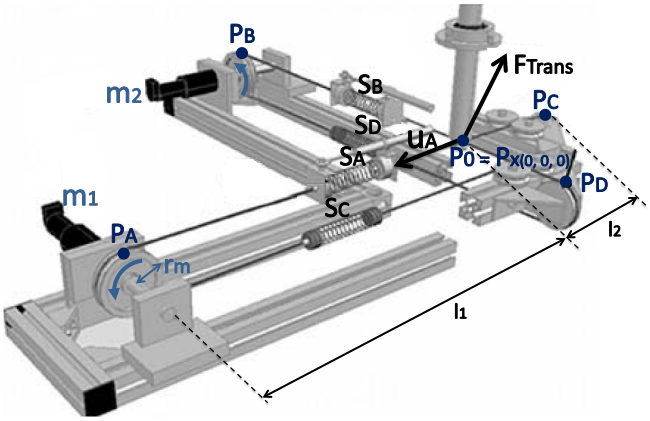

Fig. 2. SEA (Series Elastic Actuator) [19].

main arm of length $l_3 + l_4$ presents a spherical joint with respect to a fixed structure. Hence, the motion of $\mathbf{P_x}$ is constrained to the surface of a sphere of radius l_3,

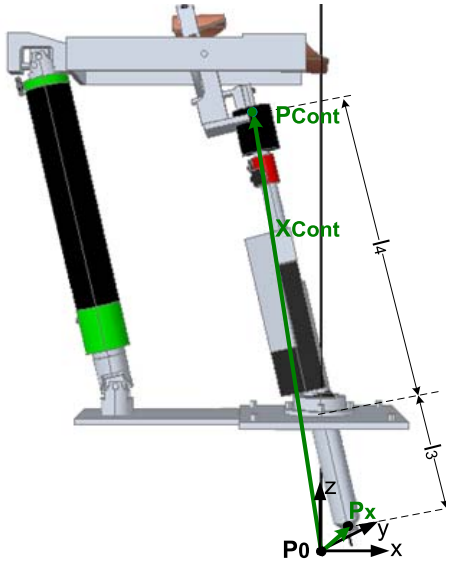

Fig. 3. Pantograph in ARM Mode [18].

$$\mathbf{P_0P_x} = \mathbf{x_{Trans}} = \begin{bmatrix} x & y & z \end{bmatrix}^T \rightarrow x^2 + y^2 + (l_3 - z)^2 = l_3^2 \quad (1)$$

The variable length of each spring n_{S_i} (Fig. 2) depends on the motors rotation angle $\mathbf{q_m} = \begin{bmatrix} q_{m_1} & q_{m_2} \end{bmatrix}^T$ and the position of the connection point $\mathbf{P_x}$, which defines the transmission displacement to the pantograph $\mathbf{x_{Trans}}$. Hence, it can be demonstrated that,

$$\begin{aligned} n_{S_A} &= l_A + q_{m_1} r_m - l_1 \\ n_{S_B} &= l_B + q_{m_2} r_m - l_1 \\ n_{S_C} &= l_C + q_{m_1} r_m - l_2 \\ n_{S_D} &= l_D + q_{m_2} r_m - l_2 \end{aligned} \quad (2)$$

where r_m is the pulley radious, l_i is the distance between $\mathbf{P_x}$ and $\mathbf{P_i}$, for $i = A,\ldots,D$, l_1 is the distance between motor axis and $\mathbf{P_0}$, and l_2 is the distance between $\mathbf{P_0}$ and the unactuated pulleys ($\mathbf{P_c}$, $\mathbf{P_D}$) (Fig. 2).

On the other hand, the force magnitude of each spring F_{Si} depends on its variable length n_{S_i}, while its direction depends on the transmission motion $\mathbf{x_{Trans}}$,

$$\mathbf{F_{Si}}(n_{S_i}, \mathbf{x_{Trans}}) = k_{S_i}\, n_{S_i}\, \mathbf{u_i} \tag{3}$$

where $\mathbf{u_i}$ is the unitary direction vector of $\mathbf{P_x P_i}$, which depends on $\mathbf{x_{Trans}}$.

Combining (2) and (3) the $i = A,B,C,D$ spring forces in function of the motors rotation angle and transmission movement is obtained.

$$\mathbf{F_{Si}}(q_{m_j}, \mathbf{x_{Trans}}) = k_{S_i}\,(l_i + q_{m_j}\, r_m - l_k)\, \mathbf{u_i} \tag{4}$$

where j is 1 for $i = A,C$ and 2 for $i = B,D$ and k is 1 for $i = A,B$ and 2 for $i = C,D$.

On the other hand, the nonlinear model of the motors $j = 1,2$ has been represented with their inertia coefficient I_{m_j}, the torsional viscous friction coefficient B_{m_j}, the Coulomb friction torque defined F_{c_j} and β_j [20],

$$\tau_{m_j} - \tau_{S_j} = I_{m_j}\, \ddot{q}_{m_j} + B_{m_j}\, \dot{q}_{m_j} + F_{c_j} \tanh(\beta_j\, \dot{q}_{m_j}) \tag{5}$$

where $\tau_{S_1} = \tau_{S_{AC}}$ in motor 1 and $\tau_{S_2} = \tau_{S_{BD}}$ in motor 2 define the equivalent torques exerted by the springs and calculated considering the forces defined in (4).

$$\begin{array}{rcl} \tau_{S_{AC}} & = & \tau_{S_A} + \tau_{S_C} = \mathbf{F_{S_A}}\, r_m + \mathbf{F_{S_C}}\, r_m \\ \tau_{S_{BD}} & = & \tau_{S_B} + \tau_{S_D} = \mathbf{F_{S_B}}\, r_m + \mathbf{F_{S_D}}\, r_m \end{array} \tag{6}$$

The transmitted force $\mathbf{F_{Trans}}$ is the sum of forces exerted by the springs in point $\mathbf{P_x}$ while the contact force $\mathbf{F_{Cont}}$ is the projection of the transmitted force to the contact point (Fig. 1).

$$\begin{array}{rcl} \mathbf{F_{Trans}} & = & \mathbf{F_{S_A}} + \mathbf{F_{S_B}} + \mathbf{F_{S_C}} + \mathbf{F_{S_D}} = \sum_{i=A}^{D} \mathbf{F_{S_i}} \\ \mathbf{F_{Cont}} & = & \mathbf{T}\, \mathbf{F_{Trans}} \end{array} \tag{7}$$

where $\mathbf{T}$ is the transformation matrix between $\mathbf{F_{Trans}}$ and $\mathbf{F_{Cont}}$ that depends on the geometry of the pantograph, the transmission motion $\mathbf{x_{Trans}}$ and the rehabilitation mode. For the particular case of the ARM mode, $\mathbf{T}$ is a simple proportional gain, which is $\mathbf{T} = l_3/l_4\, \mathbf{I}$, being $\mathbf{I}$ the identity matrix.

III. ENHANCED FORCE CONTROL DESIGN

The objective of the proposed force controller is that the SEA behaves as an ideal force generator, so that the force exerted to the user by means of the pantograph $\mathbf{F_{Des}}$ can be easily controlled by exerting proper torque references to the SEA motors τ_{m_1}, τ_{m_2}. In other words, the control objective is to make $\mathbf{F_{Cont}}$ track $\mathbf{F_{Des}}$.

For this purpose the real contact force $\mathbf{F_{Cont}}$ is required. However, direct force measurement requires the introduction of proper force sensors in the contact position, which are usually noisy. Hence, an estimator is implemented based on the dynamic model of the robot. In addition, UHP users are patients unable to control their force and motion in the first rehabilitation stages, so, the proposed force controller must be sufficiently robust to work with totally unknown perturbations.

Fig. 4 details the low level control structure proposed. This control approach is aimed to be connected to an upper level control algorithm that defines proper force references depending on the rehabilitation task to be performed. The proposed force control is composed by three cascade controllers: a speed control loop with friction compensation, a position control loop for the motors and a upper force control based on the contact force estimation and the projection of the required force to the motor motions considering the model of the robot.

Note that in order to compute the force control, the robot is equipped with several position sensors that measure the motors rotation angle $\mathbf{q_m}$ and their speed $\dot{\mathbf{q}}_\mathbf{m}$, the A and B springs variable lengths $\mathbf{n_S}$ and the inclination of the pantograph in x and y axes, which allows to estimate precisely the transmission motion $\mathbf{x_{Trans}}$. From these values, using the dynamic model, the contact force $\mathbf{F_{Cont}}$ can be estimated without using a force sensor.

The inner control loop of the proposed approach is a speed based control in which the motor dynamics is decoupled and linearized. Based on (5), the linear τ_{Es_j} and nonlinear τ_{Cm_j} torque components can be defined,

$$\begin{array}{rcl} \tau_{m_j} & = & \tau_{Es_j} + \tau_{Cm_j} \\ \tau_{Es_j} & = & I_{m_j}\, \ddot{q}_{m_j} + B_{m_j}\, \dot{q}_{m_j} \\ \tau_{Cm_j} & = & Fc_j \tanh(\beta_j\, \dot{q}_{m_j}) + \tau_{S_j} \end{array} \tag{8}$$

where τ_{S_j} depends on the transmission motion $\mathbf{x_{Trans}}$ and the motor motion $\dot{\mathbf{q}}_\mathbf{m}$.

A feedback linearization approach is used for the nonlinear coupled torque component τ_{Cm_j}, so that the linear torque τ_{Es_j} can be used to tune the PI speed controller. The linearized speed control loop is controlled by a P position control, so that the linearized decoupled system is reduced to a classical servocontrol scheme. This way, the motor control loop can be easily tuned.

The contact force $\mathbf{F_{Cont}}$ is obtained based on the spring force sum $\sum \mathbf{F_{S_i}}$ and the transmission motion $\mathbf{x_{Trans}}$. The latter is directly measured and calculated using an inclinometer while the former can be calculated in terms of the spring forces measurements $\mathbf{n_s}$ and the transmission motion $\mathbf{x_{Trans}}$, (7).

The force control is based on a PI control that compares the reference force and the estimated contact one. The controller output has to be projected to the motor control loop. For that purpose, the model that relates the motor angles and the contact force is considered. Combining (7) and (4) and solving for $\mathbf{q_m}$,

$$\mathbf{q_{Es}} = f(\mathbf{F_{Ref}}, \mathbf{x_{Trans}}) \tag{9}$$

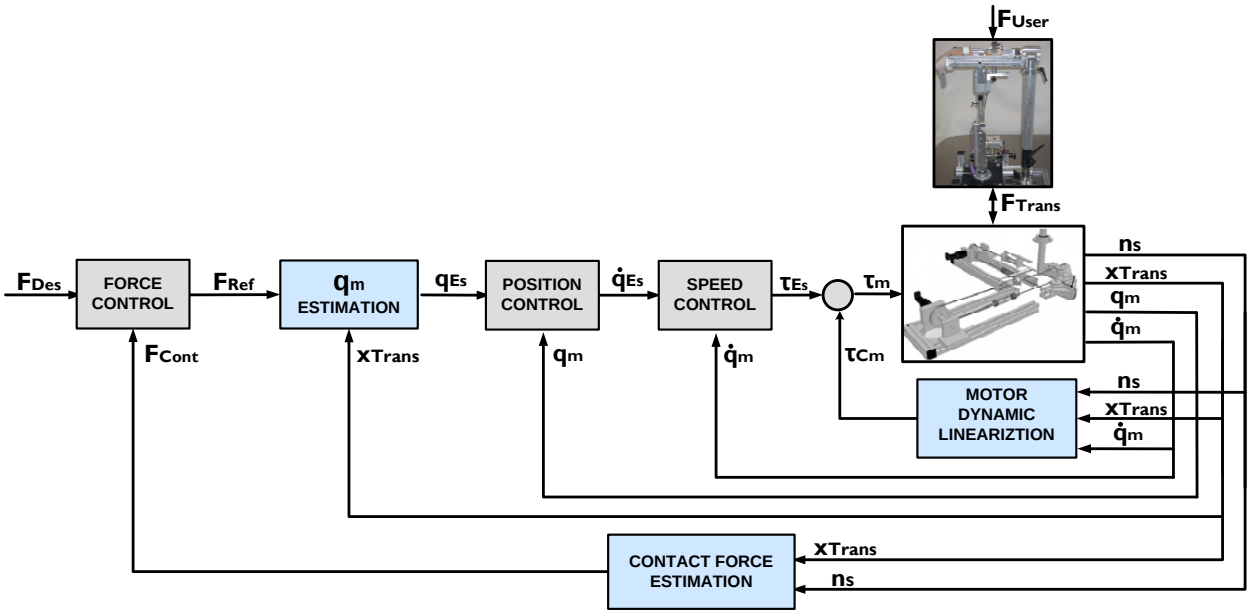

Fig. 4. Force Control Structure.

IV. VALIDATION RESULTS

Several simulation and experimental tests have been carried out to demonstrate the effectiveness of the control approach. These tests will simulate human-robot interaction, considering a series of limitations. First, it should be noted that in rehabilitation robots speed and accuracy are not critical in the controller response, but gentle and robust performance even with external perturbations.

Dynamic and geometric parameters of the UHP elements have been experimentally identified. The parameters of the motors have been identified using the Greybox procedure [20]. Real prototype parameters are summarized in Table I.

TABLE I
PARAMETERS OF THE UHP PROTOTYPE

Parameter	Value
l_1	$0.575m$
l_2	$0.15m$
l_3	$0.18m$
l_4	$0.46m$
r_m	$0.047m$
k_i	$4000N/m$
I_{m_1}	$0.003615N \cdot s^2/rad$
I_{m_2}	$0.002742N \cdot s^2/rad$
B_{m_1}	$1.02 \cdot 10^{-7} N \cdot s/rad$
B_{m_2}	$5.27 \cdot 10^{-9} N \cdot s/rad$
F_{c_1}	$0.840395Nm$
F_{c_2}	$0.731213Nm$
β_1	4223.98
β_2	4318.25

Controller parameters have been tuned for optimum performance. Speed controller (PI) has been tuned so that the resulting time constant of the linearized system be 1 ms, i.e, $T_{iv} = I_{m_i}/B_{m_i}$ and $K_{pv} = 1000 I_{m_i}$. The position controller (P) has been tuned to avoid overshoots, $K_{pp} = K_{pv}/(4 I_{m_i})$. Finally, the force controller (PI) parameters are experimentally tuned to avoid overshoot, obtaining $K_{pf} = 0.1$ (N) and $T_{if} = 0.1$ s.

Simulation tests have been carried out using Matlab/Simulink environment. For that purpose, external interaction force generated by the patient has to be implemented to simulate the behaviour. As the human interacts with the pantograph of the UHP, the human interaction has been simulated using a computed torque control model of the pantograph which includes a PD control. This human model tries to follow a position reference (the exercise to be executed) and applies the required interaction force on the pantograph to achieve this motion (Fig. 5). Parameters of the controller have been tuned to avoid overshoots ($K_p = 100$, $K_v = 20$).

Three simulated tests have been carried out to validate the controller. First, the robot position is locked and the contact force is modified, simulating a patient that tries to maintain the robot position constant. The main goal of this test is to verify that the controller works well with variable contact forces. In order to analyze this performance, the desire force $\mathbf{F_{Des}}$ is varied considering that the robot is maintained in a fixed position.

$$\begin{aligned} F_{Desx} &= 3\,(e^{-t} - 1) + sin(t) \\ F_{Desy} &= (e^{-t} - 1)\,(-2 + cos(0.5t)) \end{aligned}$$

For this particular case, the x component of $\mathbf{x_{Trans}}$ is maintained at 0.05 m, while the y axis is maintained fixed in 0.05 m.

Fig. 6 shows both the x and y components of the desired force $\mathbf{F_{Des}}$ and the contact force $\mathbf{F_{Cont}}$. As it can be seen, the controller is able to follow the desired force reference

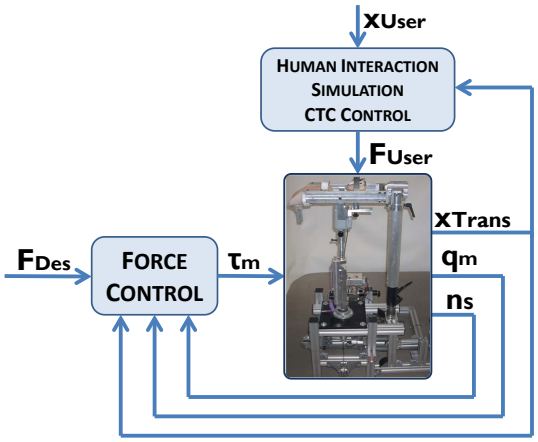

Fig. 5. Simulation Block Diagram.

changes with small errors and no overshoot, being the maximum tracking error of 0.11 N.

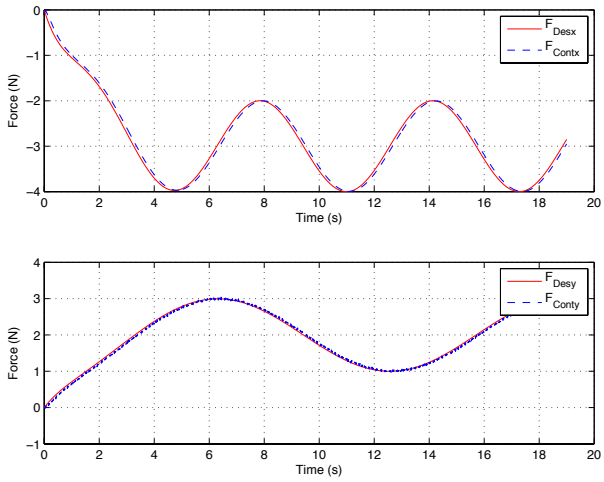

Fig. 6. First Test: Comparison between $\mathbf{F_{Des}}$ and $\mathbf{F_{Cont}}$.

The second test is used to validate the controller ability to maintain a predefined contact force when the patient moves the robot to perform the rehabilitation exercises. In order to validate the approach a constant reference of 2 N in the x axis and -3 N in the y axis is applied. With this reaction force, the patient motion is simulated with a 0.05 m radius circular trajectory.

$$\begin{aligned} x &= 0.05\,sin(t) \\ y &= 0.05\,cos(t) \end{aligned}$$

Results are shown in Fig. 7. As it can be seen, the controller tries to maintain the contact force constant in both directions, compensating the perturbation caused by the external forces exerted by the patient to execute the circular trajectory. The maximum tracking error is 0.13N in this case, obtaining an enhanced tracking over the previous controller defined in [19].

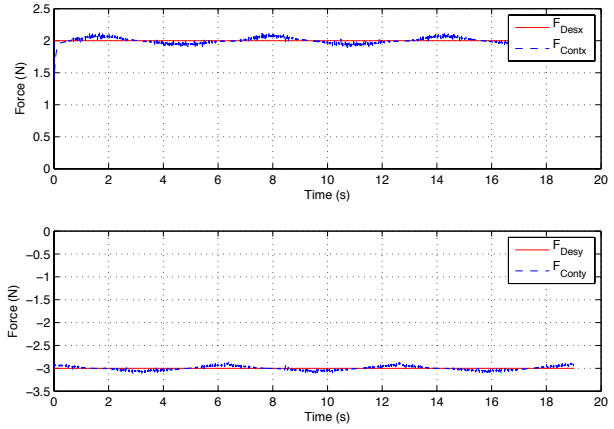

Fig. 7. Second Test: Comparison between $\mathbf{F_{Des}}$ and $\mathbf{F_{Cont}}$.

The final simulation test is used to validate the controller ability to adapt to the forces and motions exerted by the patient when force references are not constant. This simulates the most realistic case where the force reference is calculated by a high level controller that reads the motion of the patient and adapts the exerted force depending on the position and the rehabilitation procedure to be executed.

In this case, the trajectories for both the force reference and the patient motion used in the first and second cases are combined. This is, the force reference will be the one defined in the first test, while the patient position will be the one defined in the second test.

Results are shown in Fig. 8. As it can be seen, the response is similar of the one shown in Fig. 7, although small errors caused by the disturbance forces caused by the patient motion can be seen. However, tracking errors are acceptable, being the maximum one of 0.17N.

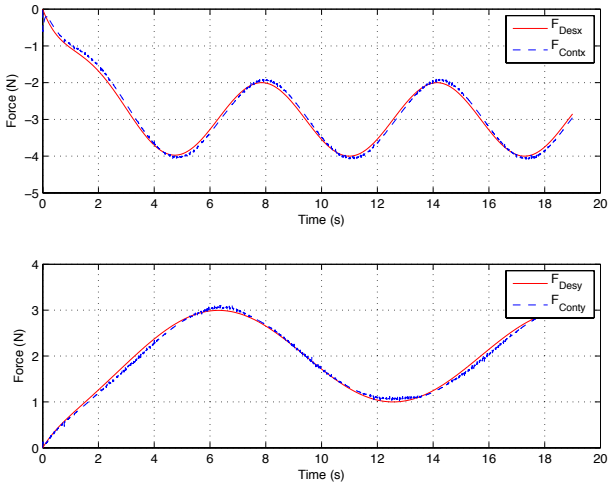

Fig. 8. Third Test: Comparison between $\mathbf{F_{Des}}$ and $\mathbf{F_{Cont}}$.

In addition to the simulated tests, an experimental test is

carried out. For that purpose, the proposed controller has been implemented in Labview Real-Time to demonstrate the validity of the approach. A 5ms force control cycle has been defined to guarantee correct haptic response. In Fig. 9 the $\mathbf{F_{Des}}$ and $\mathbf{F_{Cont}}$ forces are shown when the user tries to maintain the UHP pantograph position fixed in its origin and constant references are applied. As it can be seen, the controller performs with no overshoot and guarantees a proper force tracking, with a maximum error of 0.2N.

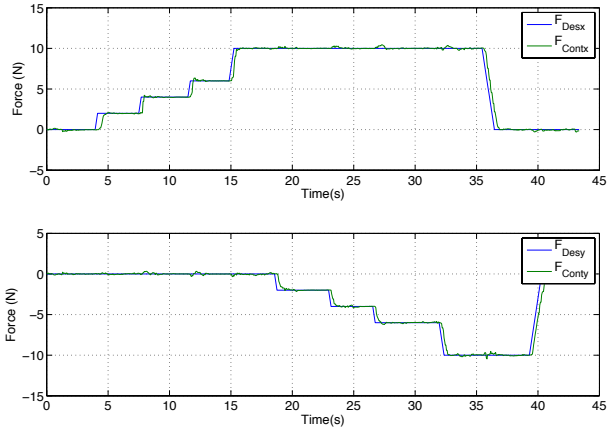

Fig. 9. Experimental Test with constant position.

V. CONCLUSIONS

In this work a new low level force control structure for rehabilitation robots is designed for the Universal Haptic Pantograph. The controller aims to control the force exerted to the patient by means of a robust model based approach.

The approach is based on a cascade based architecture, in which the coupled nonlinear equations of the Series Elastic Actuator are decoupled using a nonlinear feedback approach, and a cascade speed-position is then applied to control the position of the actuators. A model-based force-position projection is carried out to implement the force controller. Moreover, the proposed approach is based on a contact force estimation based on the model of the robot, and does not require external sensors to measure the interaction force.

To verify the performance of the design, a set of simulation and experimental test have been carried out. Results show that the controller is able to track desired force within mean tracking error of 0.1N in all relevant scenarios, without making overshoots and sudden movements which fulfills the needs of haptic performance. So, there are fulfilled all the needs of rehabilitation robots and stroke patients.

REFERENCES

[1] A. G. Thrift, D. A. Cadilhac, T. Thayabaranathan, G. Howard, V. J. Howard, P. M. Rothwell, and G. A. Donnan, "Global stroke statistic," *International Journal of Stroke*, vol. 9, no. January, pp. 6–18, 2014.

[2] C. Z., "A growing global burden," *Nature*, vol. 510, pp. 5–6, 2014.

[3] F. L. C. Lin C. H., Lien W. M. , Wang W.W. , Chen S. H. , Lo C.H., Lin S. Y., "NTUH - II Robot Arm with Dynamic Torque Gain Adjustment Method for Frozen Shoulder Rehabilitation," in *IEEE/RSJ International Conference on Intelligent Robots and Systems*, (Chicago, IL USA), pp. 3555–3560, 2014.

[4] M.-H. Milot, S. J. Spencer, V. Chan, J. P. Allington, J. Klein, C. Chou, J. E. Bobrow, S. C. Cramer, and D. J. Reinkensmeyer, "A crossover pilot study evaluating the functional outcomes of two different types of robotic movement training in chronic stroke survivors using the arm exoskeleton BONES.," *Journal of neuroengineering and rehabilitation*, vol. 10, p. 112, Jan. 2013.

[5] R. Lu, Z. Li, S. Member, C.-y. Su, and A. Xue, "Development and Learning Control of a Human Limb With a Rehabilitation Exoskeleton," *Industrial Electronics*, vol. 61, no. 7, pp. 3776–3785, 2014.

[6] W. Hassani, S. Mohammed, H. Rifaï, and Y. Amirat, "Powered orthosis for lower limb movements assistance and rehabilitation," *Control Engineering Practice*, vol. 26, pp. 245–253, May 2014.

[7] T. G. Sugar, J. He, S. Member, E. J. Koeneman, J. B. Koeneman, R. Herman, H. Huang, R. S. Schultz, D. E. Herring, J. Wanberg, S. Balasubramanian, P. Swenson, and J. A. Ward, "Design and Control of RUPERT : A Device for Robotic Upper Extremity Repetitive Therapy," *Neural Systems and Rehabilitatiom Emgineering*, vol. 15, no. 3, pp. 336–346, 2007.

[8] J. Rosen, "PID admittance control for an upper limb exoskeleton," in *American Control Conference*, (O'Farrell Street, San Francisco, CA, USA), pp. 1124–1129, Ieee, June 2011.

[9] F. Reyes, *Robótica: control de robots manipuladores*. Marcombo, S.A., 2011.

[10] A. H. Stienen, E. E. Hekman, H. T. Braak, A. M. Aalsma, F. C. Van der Helm, and H. Van der Kooij, "Design of a Rotational Hydro-Elastic Actuator for an Active," in *Biomedical Robotics and Biomechatronics*, (Scottsdale, AZ, USA), pp. 881–888, IEEE, 2008.

[11] C. Carignan, J. Tang, and S. Roderick, "Development of an Exoskeleton Haptic Interface for Virtual Task Training," in *International Conference on Intelligent Robots and Systems*, (Louis, USA), pp. 3697–3702, 2009.

[12] N. Hogan, "Impedance Control : An Approach to Manipulation," *Journal of Dynamic Systems, Measurement, and Control*, vol. 107, no. 2, pp. 1–24, 1985.

[13] T. R. Kurfess, *Robotics and Automation Handbook*. London, New York, Washington: CRC Press, 2005.

[14] R. Vertechy, A. Frisoli, A. Dettori, M. Solazzi, and M. Bergamasco, "Development of a New Exoskeleton for Upper Limb Rehabilitation," in *International Conference on Rehabilitation Robotics*, (Kyoto International Conference Center, Japan), pp. 188–193, IEEE, 2009.

[15] M. H. R. Member, T. K. Ouimet, M. S. S. Member, and J. P. Kenné, "Development and Control of a Wearable Robot for Rehabilitation of Elbow and Shoulder Joint Movements," in *Industrial Electronics Society*, pp. 1506–1511, IEEE, 2010.

[16] Z. Song, S. Zhang, and B. Gao, "Implementation of Resistance Training Using an Upper-Limb Exoskeleton Rehabilitation Device for Elbow Joint," *Journal of Medical and Biological Engineering*, vol. 34, no. 2, pp. 188–196, 2013.

[17] R. A. R. C. Gopura, K. Kiguchi, and Y. Li, "SUEFUL-7: A 7dof upper-limb exoskeleton robot with muscle-model-oriented EMG-based control," in *International Conference on Intelligent Robots and Systems*, pp. 1126–1131, Ieee, Oct. 2009.

[18] J. C. Perry, J. Oblak, J. H. Jung, I. Cikajlo, J. F. Veneman, N. Goljar, N. Bizoviar, Z. Matjačić, and T. Keller, "Variable structure pantograph mechanism with spring suspension system for comprehensive upper-limb haptic movement training," *The Journal of Rehabilitation Research and Development*, vol. 48, no. 4, p. 317, 2011.

[19] J. Oblak and Z. Matjačić, "Design of a series visco-elastic actuator for multi-purpose rehabilitation haptic device.," *Journal of neuroengineering and rehabilitation*, vol. 8, p. 3, Jan. 2011.

[20] E. Wernholt, S. Gunnarsson, and S. Link, "Nonlinear Identification of a Physically Parameterized Robot Model," (Newcastle, Australia), p. 9, SYSID, 2006.